The Thermodynamic Basis for Enantiodiscrimination: Gas-Phase Measurement of the Enthalpy and Entropy of Chiral Amine Recognition by Dimethyldiketopyridino-18-crown-6†

Yongjiang Liang, Jerald S. Bradshaw, and David V. Dearden*

Department of Chemistry and Biochemistry, Brigham Young University, C100 Benson Science Building, Provo, Utah 84602-5700

Received: February 28, 2002; In Final Form: June 22, 2002

Discrimination between the enantiomers of 1-phenylethylamine (PhEt) and α(1-naphthyl)ethylamine (NapEt) by the chiral ligand protonated dimethyldiketopyridino-18-crown-6 was studied using Fourier transform ion cyclotron resonance mass spectrometry to perform variable-temperature equilibrium (van't Hoff) experiments in the gas phase. The heterochiral complexes [(*S*,*S*)-ligand with (*R*)-amine, for example] have more-favorable enthalpy in both studied cases than the homochiral complexes; the differences are -6.7 ± 0.7 kJ mol^{-1} for the PhEt enantiomers and -10.0 ± 1.2 kJ mol^{-1} for the NapEt enantiomers. Entropy disfavors the heterochiral complexes by -14.8 ± 2.2 J mol^{-1} K^{-1} for PhEt and by -20.0 ± 3.9 J mol^{-1} K^{-1} for NapEt; entropy−enthalpy compensation is evident. These results suggest that enantiodiscrimination in these complexes is enthalpic and that locking of methyl rotors in the thermodynamically disfavored complexes is probably not important. Computational methods were also used to determine complex geometries at the HF/6-31+G* level (diffuse functions on O and N atoms only), and energies at these geometries were determined using the same basis set with MP2 and B3LYP methods. The computed geometries have shorter hydrogen-bonding distances in the heterochiral complexes than those in the homochiral ones. The computational results also correctly predict that the heterochiral complexes are energetically favored. The calculations at most levels fail to reproduce the experimental finding that enantiodiscrimination of NapEt is greater than that of PhEt.

Introduction

Many of the molecules that are the fundamental building blocks of living things are chiral, and many biochemical processes show preference for one enantiomer over the other. This remarkable ability of nature to distinguish between molecules that differ only in the arrangement of atoms around stereocenters has many practical implications. For example, a large fraction of current pharmaceuticals are chiral, and an increasing number are being marketed as single enantiomers.[1] Understanding the fundamental chemistry behind enantiodiscrimination is important. For instance, it is crucial for developing new chiral drugs and for building and improving enantiomer-specific analytical assays.

The study of enantioselectivity in the gas phase has recently been reviewed.[2] Gas-phase studies of enantiodiscrimination have direct bearing both on gaining fundamental understanding and on developing analytical techniques that can distinguish between enantiomers. In the absence of solvent, the intrinsic interactions between a guest molecule and its receptor are laid bare, and the interactions responsible for enantiodiscrimination can be studied without the masking effects that often arise from solvation.

Gas-phase studies of chiral systems generally take one of four approaches. Some are based on differences in the observed peak heights of diastereomeric complexes, which are often isotopically labeled so that they can be distinguished in a mass spectrometer. For example, the heights of mass spectrometric peaks corresponding to chiral host−chiral guest complexes generated using fast atom bombardment or electrospray have been compared to characterize enantiodiscrimination.[3,4] Similarly, observation of "magic number" homochiral serine octamers from electrosprayed solutions[5,6] has led to possible explanations for prebiotic homochirality.

Another approach examines differences in the dissociation (usually collision-induced) of diastereomers. These are often proton-bound[7] or metal ion-bound[8−10] clusters of the chiral analytes with chiral reference molecules. The success of these sensitive analytical techniques depends on differences in the extent of fragmentation observed for different analyte enantiomers in the diastereomeric clusters. Because many different reference species can be used to provide recognition of a given analyte, these methods appear to be quite general.

Differences in the reactivities of enantiomers have also been observed through measurements of reaction rates. For example, the reaction rates of protonated *sec*-butyl acetate enantiomers toward chiral tri-*sec*-butyl borates differ.[11] Similarly, the rates of chiral amine enantiomer displacement from protonated permethylated β-cyclodextrin by propylamine show strong enantiomeric dependence in many cases,[12] and this has been exploited to develop analytical methods that determine enantiomeric excess.[13,14]

Our group has focused on either host[15] or guest[16] exchange equilibrium measurements as probes of enantiodiscrimination. Our emphasis has been on understanding the fundamental interactions responsible for chiral recognition rather than on the development of analytical techniques, although we have also shown that equilibrium methods can be adapted for analysis of enantiomeric excess.[17] This prior work showed much weaker chiral recognition by the host dimethyldiketopyridino-18-crown-6 (Figure 1; hereafter referred to as host **1**) for the

† Part of the special issue "Jack Beauchamp Festschrift".

* To whom correspondence should be addressed. Phone: (801)422-2355. Fax: (801)422-0153. E-mail: david_dearden@byu.edu.

10.1021/jp025705x CCC: $22.00
Published on Web 08/23/2002

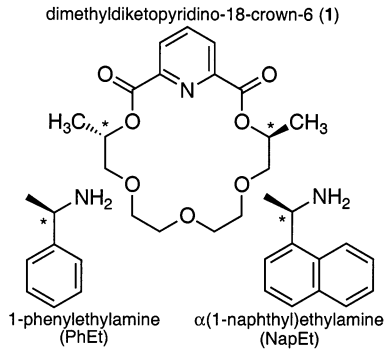

Figure 1. Structures of chiral host **1** (dimethyldiketopyridino-18-crown-6) and chiral guests 1-phenylethylamine (PhEt) and α(1-naphthyl)-ethylamine (NapEt). Stereocenters are marked with asterisks.

cyclohexylethylamine enantiomers than for the enantiomers of 1-phenylethylamine (PhEt, Figure 1). These two guests differ in that the latter is dehydrogenated and thus possesses a π system. Further, even greater enantiodiscrimination is observed for α(1-naphthyl)ethylamine (NapEt, Figure 1), a guest with a more extensive π system. From this evidence, we inferred that face-to-face stacking between the π system of the guest and the pyridino-carbonyl π system of host **1** is important in enantiodiscrimination. Examination of molecular models suggested close methyl rotor contacts in the thermodynamically less-favorable homochiral host−guest complexes, which are not present in the more-favorable heterochiral complexes. We therefore suggested that methyl rotor locking might be responsible for chiral recognition in these systems.

In this paper, we test the methyl rotor locking hypothesis by using variable-temperature equilibrium (van't Hoff) techniques to measure the enthalpic and entropic differences between diastereomeric complexes of (*S*,*S*)-**1** and (*R*,*R*)-**1** with (*R*)-PhEt and (*S*)-NapEt. If methyl rotor locking causes enantiodiscrimination, this should be apparent in more-favorable entropy for the thermodynamically favored complex. We will show that rotor locking is in fact not responsible for chiral recognition by this system; rather, enthalpy plays a key role. We will also present results from computational studies of these same complexes.

Experimental Section

All experiments were carried out in a Fourier transform ion cyclotron resonance (FTICR) mass spectrometer (model APEX 47e; Bruker Daltonics, Billerica, MA), equipped with an ion source external to a 4.7 T superconducting magnet. The FTICR trapping cell was that supplied with the instrument, a cylindrical cross section "infinity" design.[18] A commercial electrospray ionization source with a hexapole ion guide (model 10413; Analytica, Branford, MA) was adapted for microspray by replacing the 34-gauge stainless steel spray capillary with a 50 μm i.d. fused silica capillary having a tapered tip (made by grinding with diamond grit) and exchanging the manufacturer's glass capillary vacuum interface with a heated type 316 stainless steel desolvating tube (0.0625 in. o.d. × 0.020 in. i.d.). The spray capillary was coupled with a stainless steel zero dead volume union (Valco, Houston, TX) to Teflon tubing, which makes a friction fit to a glass syringe. Typically, about 1.2 kV was applied through the zero dead volume union to the spray capillary, and flow rates of 10 μL h^{-1} were used. A zoom microscope (about 100 magnifying power) was set up near the spray capillary to monitor spray conditions. A home-built implementation of stored wave-form inverse Fourier transform (SWIFT)[19,20] was used to isolate selected ions.

The test reactions, involving proton-transfer equilibria between amines, were studied using chemical ionization in the trapping cell of the FTICR instrument, followed by SWIFT isolation of the reactant of interest. The isolated protonated amine was allowed to react with the mixture of two neutral amines in the trapping cell until proton-transfer equilibrium was attained. The procedure was then repeated by isolating the other protonated amine and allowing it to react with both neutrals until equilibrium was attained. The criteria used to establish the achievement of equilibrium have been discussed.[21,22] The amines used were triethylamine (reagent grade, Fisher), trimethylamine (anhydrous, Eastman), 1,4-diaminobutane (99%, Aldrich), and diethylamine (99%, Spectrum). All compounds were used as supplied without further purification, with the exception that the amines were degassed through three or more freeze−pump−thaw cycles before being introduced into the vacuum chamber.

The experimental techniques used to measure equilibrium constants in the chiral systems have been described.[16,17] In brief, one enantiomer of the host molecule was electrosprayed (0.1 mg/mL in 80:18:2 methanol/water/acetic acid), generating protonated host ions. Pure enantiomers of host **1** were prepared using published procedures.[23] In some experiments, the achiral host 18-crown-6 (18C6, Sigma) was used instead. The neutral, chiral amine of interest [(*R*)-1-phenylethylamine (>98%, Fluka) or (*S*)-α(1-naphthyl)ethylamine (>99%, Fluka)] was introduced into the ion trapping cell region via a controlled variable leak valve to a stable pressure. An achiral amine, which serves as a reference, was also leaked into the instrument through a second controlled variable leak valve. The reference amine was cyclohexylamine (97.9%, Fisher) in all cases. The pressures of the two amines were maintained at a constant value throughout the experiment. Typically, the total pressure was 1×10^{-7} mbar, measured using an uncorrected cold cathode gauge (Balzers).

The reactions involved in studying the chiral systems are listed below. In practice, the entire experiment was carried out by first electrospraying one of the host enantiomers [(*R*,*R*)-**1** or (*S*,*S*)-**1**] with a constant pressure of the chiral amine of interest [(*R*)-amine or (*S*)-amine; (*R*)-amine in the reactions below] and of the reference amine (Ref) present in the trapping region of the instrument. Equilibrium populations of the ionic reactant and product of reaction 1a were measured as reflected in their

$$(R)\text{-amine}\cdot(R,R)\text{-}\mathbf{1}H^+ + \text{Ref} \rightleftarrows \text{Ref}\cdot(R,R)\text{-}\mathbf{1}H^+ + (R)\text{-amine} \quad (1a)$$

peak heights. The host molecule was then flushed from the electrospray source, and the other enantiomer was electrosprayed. The rest of the experiment is carried out in exactly the same way as for the original enantiomer, resulting in an equilibrium constant for reaction 1b. Addition of reactions 1a

$$\text{Ref}\cdot(S,S)\text{-}\mathbf{1}H^+ + (R)\text{-amine} \rightleftarrows \text{Ref} + (R)\text{-amine}\cdot(S,S)\text{-}\mathbf{1}H^+ \quad (1b)$$

and 1b yields reaction 1. Reaction 1 has the important advantage

$$(R)\text{-amine}\cdot(R,R)\text{-}\mathbf{1}H^+ + \text{Ref}\cdot(S,S)\text{-}\mathbf{1}H^+ \rightleftarrows \text{Ref}\cdot(R,R)\text{-}\mathbf{1}H^+ + (R)\text{-amine}\cdot(S,S)\text{-}\mathbf{1}H^+ \quad (1)$$

that its equilibrium constant depends only on the intensities of the measured ion signals and not on partial pressures of the neutrals,[16] which are difficult to accurately measure, particularly in variable-temperature experiments in which outgassing rates

may vary. Because the complexes Ref·(*R*,*R*)-**1**H$^+$ and Ref·(*S*,*S*)-**1**H$^+$ are enantiomers, they are thermochemically identical, so the thermochemistry of reaction 1 measures the difference between the diastereomers, (*R*)-amine·(*R*,*R*)-**1**H$^+$ and (*R*)-amine·(*S*,*S*)-**1**H$^+$, or the analogous (*S*)-amine complexes.

The equilibrium constants for reactions 1a and 1b were determined from the ratio of the peak intensities of reactant and product ions and the measured partial pressures of the two neutral reactants, as has been discussed.[15,16] As noted above, the pressure ratios cancel for reaction 1. We use absolute signal intensities as a measure of ion populations in the trapping cell; this approach has been shown to be a reasonable one.[24] The masses of the diastereomers are identical and within 80 *m*/*z* of those of the reference complexes, so no corrections have been made for possible mass discrimination. The attainment of equilibrium was verified for all reactions both by monitoring them until the reactant/product ratio became constant and by approaching this point from both the "forward" and "reverse" directions, ensuring that the same results are obtained regardless of the direction of approach.

Variable temperature experiments required a slight modification of the vacuum bake out electronics of the instrument. A single 220 V, 100 W heater band (supplied with the APEX 47e) was placed around the outside of the vacuum chamber surrounding the ion trapping cell. Copper−constantan thermocouples were mounted on ceramics immediately in contact with the trapping plates of the instrument both on the side facing the preamplifier and on the opposite side, facing the ion source. An OMEGA model CN 9000A temperature controller (OMEGA; Stamford, CT) was connected to the thermocouple on one trapping plate, while a Watlow model CL-505A temperature controller was used as a readout for the thermocouple on the other trapping plate. The OMEGA controller was used to switch the heating circuit on and off. Each readout, precise to the nearest 0.1 K, was monitored throughout each experiment to ensure the temperature gradient across the trapping cell remained less than 2 K through the duration of the experiment. Approximately 2 h was required to achieve small temperature gradients after changing the temperature setting. Stable temperatures up to 373 K were achieved with this configuration.

Conformational searches were done using MacroModel, version 6.5 (Schrödinger, Inc., Portland, OR). For each diastereomer, Monte Carlo searches were conducted with 30 000 starting structures with both the AMBER* and MMFF94s force fields supplied in MacroModel. The minimum energy conformers from the MMFF94s conformational searches (which were essentially identical to the minima found with AMBER*) were used as starting points for ab initio calculations using the Gaussian 98 suite of programs (Gaussian, Inc.; Pittsburgh, PA). Full geometry optimizations were carried out at the Hartree−Fock level with 6-31G* basis sets on all atoms except O and N, which were augmented with diffuse functions (6-31+G*). A similar approach has been taken in extensive calculations on crown ether−alkali metal cation systems.[25−28] The optimized structures were subsequently used for single-point MP2 and B3LYP energy calculations also with Gaussian 98. Because the calculations compared energies of diastereomers, we assumed that errors arising from zero-point corrections and basis set superposition would be negligible, and no corrections were made. Generally, these assumptions are good ones when calculating enantiodiscrimination.[29]

Results

Equilibrium Experiments. For a particular temperature *T*, the free energy change for a reaction is given by $\Delta G^\circ = \Delta H^\circ - T\Delta S^\circ$ and $\Delta G^\circ = -RT \ln K$, where *R* is the ideal gas constant and *K* is the equilibrium constant. It follows that a plot of $\Delta G^\circ/T$ vs $1/T$ (a van't Hoff plot) should yield a straight line with slope ΔH° and intercept $-\Delta S^\circ$.

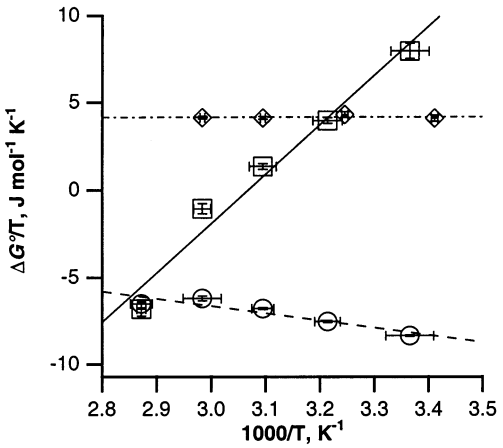

Figure 2. Van't Hoff plots for test reactions. Error bars in the *y* direction represent one standard deviation from three or more replicate measurements; error bars in the *x* direction indicate measured temperature differences between the thermocouples mounted on the two trapping plates. The lines are linear least-squares fits to the data. Circles represent $(CH_3)_3NH^+ + (C_2H_5)_2NH \rightleftarrows (CH_3)_3N + (C_2H_5)_2NH_2^+$. Squares represent $[H_2N(CH_2)_4NH_2]H^+ + (C_2H_5)_3N \rightleftarrows H_2N(CH_2)_4NH_2 + (C_2H_5)_3NH^+$. Diamonds represent 18C6H$^+$·cyclohexylamine + 1-phenylethylamine $\rightleftarrows$ 18C6H$^+$·(1-phenylethylamine) + cyclohexylamine.

TABLE 1: Thermochemical Data from van't Hoff Experiments[a]

	ΔH°, kJ mol^{-1}		ΔS°, J mol^{-1} K^{-1}	
reaction[b]	this work	lit.[c]	this work	lit.[c]
2	-4.2 ± 0.9	-3.7	-5.9 ± 2.9	-6.8
3	28.3 ± 3.0	22.6	86.9 ± 9.3	69.3 ± 5.0
4	0.02 ± 0.04	*d*	-4.1 ± 0.1	*d*
1, amine = (*R*)-PhEt	-6.7 ± 0.7	*d*	-14.8 ± 2.2	*d*
1, amine = (*R*)-NapEt	-10.0 ± 1.2	*d*	-20.0 ± 3.9	*d*

[a] Reported error limits are standard errors from linear least-squares fitting of experimental data and averaging of multiple runs. [b] See text. [c] Reference 30; errors as reported therein. [d] Not available.

Reactions 2−4 were studied to test our experimental setup

$$(CH_3)_3NH^+ + (C_2H_5)_2NH \rightleftarrows (CH_3)_3N + (C_2H_5)_2NH_2^+ \quad (2)$$

$$[H_2N(CH_2)_4NH_2]H^+ + (C_2H_5)_3N \rightleftarrows H_2N(CH_2)_4NH_2 + (C_2H_5)_3NH^+ \quad (3)$$

$$18C6H^+\cdot\text{cyclohexylamine} + \text{1-phenylethylamine} \rightleftarrows 18C6H^+\cdot\text{(1-phenylethylamine)} + \text{cyclohexylamine} \quad (4)$$

for variable-temperature equilibrium measurements. Figure 2 is a van't Hoff plot obtained under low pressure FTICR/MS conditions for reactions 2−4. The plots are linear over the accessible temperature range for all three reactions, the most likely sources of error being temperature gradients across the trapping cell during the experiments and uncertainty in measurements of the pressure ratios for the neutral species. Thermochemical information extracted from the figure is compiled in Table 1. Reaction 2 is found to be slightly exothermic with a small negative entropy change, whereas reaction 3 is entropically driven: endothermic, with a large positive entropy change. Reaction 4 involves the displacement of cyclohexylamine from

TABLE 2: Comparison of Computational and Experimental Energy Results[a]

guest amine in (*S,S*)-**1** complex	level of theory					expt[b]
	AMBER*[c]	MMFF94s[c]	HF[d]	MP2[d]	B3LYP[d]	
(*R*)-PhEt	−83.67	512.57	−1599.9063[e]	−1604.7110[e]	−1609.6594[e]	
(*S*)-PhEt	−80.80	522.18	−1599.9033[e]	−1604.7068[e]	−1609.6554[e]	
Δ[(*S,S*)-**1**·(*R*)−(*S,S*)-**1**·(*S*)]	−2.9	−9.6	−7.9	−11.1	−10.5	−6.7 ± 0.7
(*R*)-NapEt	−63.80	567.46	−1752.5534[e]	−1757.8680[e]	−1763.2955[e]	
(*S*)-NapEt	−61.61	578.01	−1752.5501[e]	−1757.8649[e]	−1763.2918[e]	
Δ[(*S,S*)-**1**·(*R*)−(*S,S*)-**1**·(*S*)]	−2.2	−10.6	−8.7	−8.0	−9.8	−10.0 ± 1.2

[a] All units are kJ mol^{-1}, except as noted. [b] Measured $\Delta H°$ for reaction 1. [c] Strain energies for the complexes. [d] Total ab initio energy obtained using 6-31G* basis set on all atoms except N and O, which were augmented with diffuse functions (6-31+G* basis set on these atoms). [e] Hartrees.

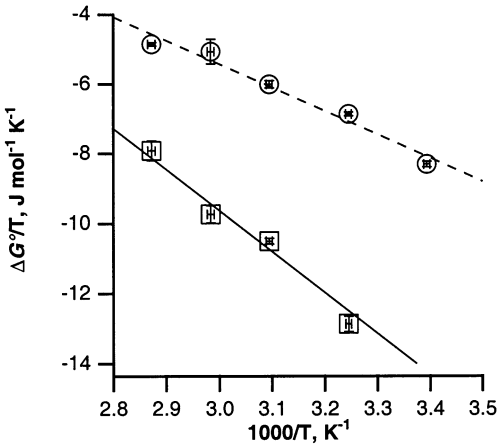

Figure 3. Van't Hoff plots for chiral recognition reactions: (*R*)-amine·(*R,R*)-**1**H$^+$ + Ref·(*S,S*)-**1**H$^+$ ⇄ Ref·(*R,R*)-**1**H$^+$ + (*R*)-amine·(*S,S*)-**1**H$^+$. Error bars in the *y* direction represent one standard deviation from three or more replicate measurements; error bars in the *x* direction indicate measured temperature differences between the two trapping plates. The lines are linear least-squares fits to the data. Ref = cyclohexylamine. Circles represent amine = (*R*)-1-phenylethylamine. Squares represent amine = (*R*)-α(1-naphthyl)ethylamine.

Figure 4. Superimposed structures (from HF/6-31+G* calculations) of (*R*)-1-phenylethylamine·(*R,R*)-**1**H$^+$ (wire frame) and (*S*)-1-phenylethylamine·(*R,R*)-**1**H$^+$ (tubes). Grey = carbon, red = oxygen, blue = nitrogen, and green = hydrogen. The guest sits deeper in the host cavity for the heterochiral complex.

protonated 18C6 by 1-phenylethylamine, one of the chiral amines that we wish to characterize. Analysis of the van't Hoff plot indicates negligible enthalpy change for this reaction (Table 1) and a small negative entropy change.

Figure 3 presents variable-temperature equilibrium results for exchanges of chiral and achiral guests between the enantiomers of the protonated chiral host, **1**H$^+$, for both chiral guests, PhEt and NapEt (reaction 1). The data at ambient temperature are in excellent agreement with earlier amine-exchange[16] and ligand-exchange[15] equilibrium measurements. For each guest, the van't Hoff plot is linear over the temperature range examined. The enthalpy and entropy changes extracted from the data are given in Table 1. Neutral pressures do not play a role in reaction 1 as long as the pressure is constant for the duration of the experiment, which is likely true because the equilibrium constants did not drift with time. Mass discrimination and inaccuracies in measuring the reactant and product peak heights are a possible source of error, but these errors are not likely to be large for closely spaced masses such as were involved here. Reaction 1, which is written in the direction of formation of the more-stable heterochiral complex, is enthalpically favorable and entropically unfavorable, more so for the guest with the larger π system.

Computational Results. The energies of the complexes, as well as the differences in energies of the diastereomeric pairs, computed at various levels of theory, are summarized in Table 2. Whereas the absolute energies for the molecular mechanics calculations have little physical meaning, the *differences* between the energies of the diastereomers should reflect differences in the stabilities of the complexes. The two molecular mechanics force fields and all levels of ab initio theory find the heterochiral (*S,S*)·*R* complexes to be more stable than the corresponding homochiral (*S,S*)·*S* complexes, in agreement with the van't Hoff experiments. Somewhat surprisingly (and perhaps fortuitously), the magnitudes of the energy differences between the two complexes are also in good agreement with experiment, even for the molecular mechanics calculations. All levels of ab initio theory give results within 2 kJ mol^{-1} of experiment for the NapEt complexes. Agreement between theory and experiment is worse for the PhEt complexes but is still reasonable (3.4 kJ mol^{-1} in the worst ab initio case); surprisingly, the largest differences are for the theoretical methods that include effects of electron correlation, MP2 and B3LYP.

The structures of the two PhEt complex diastereomers are shown superimposed in Figure 4, and a few geometric parameters from the computed PhEt and NapEt complex structures are listed in Table 3. The host crown ether adopts almost the same conformation in all of the complexes. However, the placement of the ammonium guest varies significantly in the complexes, as can be seen from the results in Table 3. The energetically favored heterochiral complexes exhibit larger angles between the planes defined by the aromatic rings of the guest and host and larger distances between the geometric centroids defined by the atoms of the guest and host aromatic rings than their homochiral counterparts. The distance from the guest ammonium nitrogen to the mean plane of the host donor atoms is shorter for the heterochiral complexes by about 0.02 Å.

TABLE 3: HF/6-31+G* Geometric Parameters for HF/6-31+G* Structures[a]

guest amine in (*S*,*S*)-**1** complex	$\pi-\pi$ angle[b]	π-centroid distance[c]	N−donor atom plane distance[d]
(*R*)-PhEt	27.05	4.7863	1.276
(*S*)-PhEt	22.06	4.3428	1.294
(*R*)-NapEt	25.43	4.3504	1.294
(*S*)-NapEt	20.02	4.1094	1.316

[a] 6-31+G* basis set on all atoms except C, which was described with the 6-31G* basis set. [b] Angle between mean plane of guest aromatic ring and host pyridino ring, deg. [c] Distance between centroids of guest aromatic ring and host pyridino ring, Å. [d] Distance between N atom of guest and mean plane of host donor atoms, Å.

Discussion

Validation of Variable-Temperature Equilibrium Methods. We tested our variable-temperature equilibrium experiment against the results of two previously studied systems, as well as for a host−guest system similar to that involving the chiral hosts and guests of interest. Bowers et al.[30] examined the equilibria of reactions 2 and 3 at variable temperatures under low-pressure conditions using ion cyclotron resonance techniques. Reaction 2 involves a simple exothermic proton transfer wherein the expected entropy change is just that arising from the change in symmetry, whereas reaction 3 involves a significant positive entropy change because protonated 1,4-diaminobutane is cyclic and decyclizes upon loss of the proton. Reaction 4 involves a guest exchange on protonated 18C6, similar to those we use to study the chiral systems of interest.

Both the $\Delta H°$ and $\Delta S°$ values (Table 1) for reactions 2 and 3 are in excellent agreement with the measurements of Bowers et al.[30] Similarly, the value of $\Delta S°$ measured for reaction 2 is in close agreement with the value expected on the basis of symmetry change in the reaction, 6.0 J mol^{-1} K^{-1}.[30]

Although to our knowledge reaction 4 has not been characterized previously, the results are consistent with what might be expected for such a system. Similar binding enthalpies to the crown should be observed for both cyclohexylamine and 1-phenylethylamine (to a first approximation) because by analogy with complexes of simpler ammonium ions with 18C6[31−34] both are expected to form three hydrogen bonds in tripodal fashion. The entropy change for the reaction can also be simply estimated. There is no symmetry change, but the available phase space for the two complexes is likely different: because 1-phenylethylamine is somewhat more sterically crowded around the amine group, we expect less flexibility in the complex of this amine than in that of cyclohexylamine. Hence, formation of the 1-phenylethylamine complex should be slightly unfavorable entropically. The experimental results in Table 1 are consistent with these predictions. Reaction 4 proceeds with no enthalpy change and a small, unfavorable entropy change as expected. In summary, our experimental setup produced results in excellent agreement with previous work, both for a reaction in which the entropy change is very small and for another in which the entropy change is large. In addition, it gave results consistent with reasonable expectations for guest exchange on unsubstituted 18C6. In combination with the results for the model proton-transfer systems, we believe this provides strong validation for our method.

Comparison of Experimental and Computational Results. All of the computational methods agree with experiment in predicting the heterochiral complexes to be lower in energy than the homochiral complexes. However, the agreement is not as good when the results for PhEt and NapEt are compared with each other. The experimental values for $\Delta H°$ (Table 2) clearly show less discrimination between the PhEt enantiomers than between those of NapEt. Of the computational methods, only molecular mechanics with the MMFF94s force field and ab initio Hartree−Fock calculations agree with this order. Interestingly, when the effects of electron correlation are included in the calculation (using either MP2 perturbation theory or B3LYP density functional methods), discrimination is predicted to be greater for the PhEt enantiomers than for the NapEt enantiomers.

Why do the experimental and computational results disagree about which amine exhibits greater enantiodiscrimination? It is not likely that the experimental results are in error; they are consistent for multiple runs done on different days under different pressure conditions. Shortcomings in the calculations are more likely; the experimental difference is only about 3 kJ mol^{-1}, and even very good computational methods often struggle to achieve this level of accuracy. Zero-point corrections to the calculations cannot account for the differences because the diastereomers should have essentially the same zero-point energies. Basis set superposition error should also be similar for the diastereomers.

The approach that we took was to compare only the lowest energy conformers, but because these are floppy complexes, it is likely that a number of conformers are thermally populated and accurate description of the system would require statistical averaging.[29] It is also likely that the basis set employed is not sufficient to compute energies accurately enough to measure the small differences observed between these systems. Calculations with larger basis sets might yield light on this issue but will be challenging for systems as large as these complexes.

Thermodynamic Basis for Enantiodiscrimination by Dimethyldiketopyridino-18-crown-6. The results for reaction 1, given in Table 1, shed light on the thermodynamic basis for discrimination between chiral amines by ligand **1**. As we noted in an earlier publication,[16] close contact occurs between host and guest methyl groups in the homochiral complexes but is absent in the heterochiral complexes. If methyl rotor locking due to the close contact were responsible for enantiodiscrimination, we would expect to see entropy favoring the heterochiral complex. However, the van't Hoff results clearly show that entropy works against binding in the favored heterochiral complexes. Instead, enantiodiscrimination in the systems that we studied is enthalpically derived.

So why is the enthalpy more favorable for the heterochiral complexes? Three types of interaction are possible between the host and guest: hydrogen bonding involving the guest ammonium group and host heteroatoms, $\pi-\pi$ stacking interactions between the aromatic π system of the guest and the pyridinocarbonyl π system of the host, and van der Waals contacts between guest and host. Any of these interactions can be either attractive or repulsive, and of course, the interactions are not independent; the complexes adopt conformations that maximize the attractive interactions while minimizing repulsions.

One possibility is that $\pi-\pi$ stacking is more attractive in the heterochiral complexes than in the homochiral ones. The experimental results suggest this might be the case; the enthalpic recognition of the heterochiral guest increases as the extent of the π system increases in going from PhEt to NapEt. The computational structures, however, cast doubt on this explanation. If differences in face-to-face π stacking interactions were responsible for the differences in enthalpies of binding the amine enantiomers, we would expect the guest and host π systems to be more parallel and to lie closer together for the favored enantiomer. The results of Table 3 show the opposite to be the case: the angles between the guest and host π systems are about

TABLE 4: HF/6-31+G* Computed Hydrogen Bond Distances[a]

guest amine in (*S*,*S*)-**1** complex	H−heteroatom distance, Å			
	1	2	3	mean
(*R*)-PhEt	2.058	2.020	1.951	2.010
(*S*)-PhEt	2.085	2.209	2.041	2.112
(*R*)-NapEt	2.046	1.970	2.028	2.015
(*S*)-NapEt	2.090	2.042	2.210	2.114

[a] 6-31+G* basis set on all atoms except C, which was described with the 6-31G* basis set.

5° greater for the heterochiral complexes, and the centroids of the two π systems are farther apart than for the homochiral complexes. Thus, according to theory, differences in π stacking interactions in the systems that we studied do not appear to account for the observed differences in binding enantiomers.

The computational results do allow the possibility that the importance of $\pi-\pi$ stacking in complexes of host **1** increases as the π systems become more extensive. Table 3 indicates that the $\pi-\pi$ angles are less in the NapEt complexes than in the PhEt complexes and that the π systems are also closer together in the NapEt complexes. Another way to test the importance of $\pi-\pi$ stacking is to use substituents to vary the π electron density in the guest aromatic ring, and equilibrium experiments based on these ideas are currently underway.

If π stacking does not account for enantiodiscrimination by host **1**, then perhaps differences in the abilities of the two guest enantiomers to form hydrogen bonds with the host, mediated by differences in van der Waals contacts, are responsible. Superior hydrogen bonding should be evident in shorter bond lengths and more linear donor−H−acceptor angles. According to the computed structures, hydrogen bonding is clearly more favorable for the enthalpically favored, heterochiral complexes. The distances between the guest hydrogens and the host heteroatoms (Table 4) average about 0.1 Å shorter for the heterochiral complexes. Similarly, the computed hydrogen bond angles (not shown) are more linear for the heterochiral complexes.

Entropy−Enthalpy Compensation. Comparison of the results for the PhEt and NapEt complexes shows enthalpy−entropy compensation[35−38] as is commonly seen in host−guest systems: more-favorable enthalpy leads to tighter host−guest binding, leading to a reduction in the flexibility of the resulting complex and therefore to less-favorable entropy of complexation. Thus, recognition of (*R*)-NapEt by (*S*,*S*)-**1** is about 3 kJ mol^{-1} *more* favorable enthalpically than recognition of (*R*)-PhEt but about 5 J mol^{-1} K^{-1} *less* favorable entropically. Similar effects have been observed in other host−guest systems involving $\pi-\pi$ stacking interactions in the binding of arene guests by cyclophanes[36] and in cyclodextrin complexes with carboxylate guests,[38] but all prior studies were carried out in condensed media and solvation effects were dominant. To our knowledge this is the first case in which enthalpy−entropy compensation has been characterized for a host−guest system in the gas phase, with bulk solvent interactions playing no role.

Effect of Solvation on Enantiodiscrimination. The thermochemistry of recognition of the NapEt enantiomers by **1** has been studied in methanol solution,[39] facilitating comparison with the gas-phase results. The comparison reveals the influence of solvation on enantiodiscrimination. The enthalpic difference between the diastereomers is -10 ± 1.2 kJ mol^{-1} in the gas phase but only $^1/_{10}$ as great in solution (-1.1 ± 0.5 kJ mol^{-1}). The trends in enthalpy with solvation are easily rationalized. Solvation competes with the direct host−guest interaction. To the extent that either host or guest is solvated by an achiral solvent such as methanol, their direct interaction with each other is weakened and the degree of enantiodiscrimination decreases. This effect is quite large for methanol solvation of the NapEt-**1** guest−host system.

The trends in entropy are more difficult to understand than those in enthalpy, but again the competition between solvation and direct host−guest interaction comes into play. For reaction 1 with NapEt guests in the gas phase, $\Delta S°$ is -20.0 ± 3.9 J mol^{-1} K^{-1}, reflecting entropy−enthalpy compensation as noted above. In methanol solution, on the other hand, the same entropic difference is only $^1/_5$ as large and in the opposite direction (+4.1 J mol^{-1} K^{-1}). In the gas phase, the more-favorable diastereomer is more-tightly bound and therefore more-ordered than the less-favorable one, as indicated by the negative entropy difference. In solution, the system is more complicated because it includes solvent molecules in addition to the host−guest complex. The enthalpically favored complex is also entropically favored in solution, implying greater disorder for the heterochiral system. If the heterochiral host and guest are more-tightly associated as indicated by the gas-phase results, they likely interact less well with the solvent than do the components of the homochiral complex, and the resulting decrease in solvent ordering more than makes up for the tighter complexation. The net change due to loss of order in the solvent would account for the entropic favorability of the heterochiral system in methanol.

Conclusions

Our original hypothesis, that enantiodiscrimination in these systems is entropic, is incorrect. Rather, chiral recognition of PhEt and NapEt enantiomers by chiral crown ether host **1** occurs because the enthalpy of binding is more favorable for the favored enantiomers, probably because of decreased steric repulsions allowing better hydrogen bonding between the guest and the host. The intrinsic entropy of the recognition reaction actually works against the favored enantiomers, as expected based on entropy−enthalpy compensation. Computational modeling of accurate energies for these relatively large host−guest complexes remains challenging; it is still possible to achieve greater accuracy with experiments than with easily accessible calculations.

The role of π stacking in enantiodiscrimination by **1** remains ambiguous. Trends of increasing discrimination with increasing π system extent suggest stacking is important, but two similar guests studied with the same host hardly constitute an extensive trend; studies with additional guests are needed. Computed structures show the guest and host π systems are not parallel. Additional experimental work designed to address this issue is now underway.

Acknowledgment. We are grateful for support of this work by the donors of the Petroleum Research Fund, administered by the American Chemical Society, and by the National Science Foundation. We are also grateful for the computational resources supplied by the Ira and Mary Lou Fulton Supercomputing Center at Brigham Young University and for the assistance of Professor Matt Asplund with the computational work.

References and Notes

(1) Stinson, S. C. *Chem. Eng. News* **2000**, *78*, 55−78.

(2) Filippi, A.; Giardini, A.; Piccirillo, S.; Speranza, M. *Int. J. Mass Spectrom.* **2000**, *198*, 137−163.

(3) Sawada, M. *Mass Spectrom. Rev.* **1997**, *16*, 73−90.

(4) Sawada, M.; Takai, Y.; Yamada, H.; Nishida, J.; Kaneda, T.; Arakawa, R.; Okamoto, M.; Hirose, K.; Tanaka, T.; Naemura, K. *J. Chem. Soc., Perkin Trans. 2* **1998**, 701−710.
(5) Cooks, R. G.; Zhang, D.; Koch, K. J.; Gozzo, F. C.; Eberlin, M. N. *Anal. Chem.* **2001**, *73*, 3646−3655.
(6) Julian, R. R.; Hodyss, R.; Kinnear, B.; Jarrold, M. F.; Beauchamp, J. L. *J. Phys. Chem. B* **2002**, *106*, 1219−1228.
(7) Yao, Z.-P.; Wan, T. S. M.; Kwong, K.-P.; Che, C.-T. *Chem. Commun.* **1999**, 2119−2120.
(8) Tao, W. A.; Wu, L.; Cooks, R. G. *Chem. Commun.* **2000**, 2023−2024.
(9) Tao, W. A.; Zhang, D.; Nikolaev, E. N.; Cooks, R. G. *J. Am. Chem. Soc.* **2000**, *122*, 10598−10609.
(10) Tao, W. A.; Gozzo, F. C.; Cooks, R. G. *Anal. Chem.* **2001**, *73*, 1692−1698.
(11) Filippi, A.; Speranza, M. *Int. J. Mass Spectrom.* **2000**, *199*, 211−219.
(12) Lebrilla, C. B. *Acc. Chem. Res.* **2001**, *34*, 653−661.
(13) Grigorean, G.; Ramirez, J.; Ahn, S. H.; Lebrilla, C. B. *Anal. Chem.* **2000**, *72*, 4275−4281.
(14) Grigorean, G.; Lebrilla, C. B. *Anal. Chem.* **2001**, *73*, 1684−1691.
(15) Chu, I.-H.; Dearden, D. V.; Bradshaw, J. S.; Huszthy, P.; Izatt, R. M. *J. Am. Chem. Soc.* **1993**, *115*, 4318−4320.
(16) Dearden, D. V.; Dejsupa, C.; Liang, Y.; Bradshaw, J. S.; Izatt, R. M. *J. Am. Chem. Soc.* **1997**, *119*, 353−359.
(17) Liang, Y.; Bradshaw, J. S.; Izatt, R. M.; Pope, R. M.; Dearden, D. V. *Int. J. Mass Spectrom.* **1999**, *185/186/187*, 977−988.
(18) Caravatti, P.; Allemann, M. *Org. Mass Spectrom.* **1991**, *26*, 514−518.
(19) Chen, L.; Marshall, A. G. *Int. J. Mass Spectrom. Ion Processes* **1987**, *79*, 115−125.
(20) Chen, L.; Wang, T.-C. L.; Ricca, T. L.; Marshall, A. G. *Anal. Chem.* **1987**, *59*, 449−454.
(21) Operti, L.; Tews, E. C.; Freiser, B. S. *J. Am. Chem. Soc.* **1988**, *110*, 3847−3853.
(22) Chen, Q.; Cannell, K.; Nicoll, J.; Dearden, D. V. *J. Am. Chem. Soc.* **1996**, *118*, 6335−6344.
(23) Jones, B. A.; Bradshaw, J. S.; Izatt, R. M. *J. Heterocycl. Chem.* **1982**, *19*, 551−556.
(24) Goodner, K. L.; Milgram, K. E.; Williams, K. R.; Watson, C. H.; Eyler, J. R. *J. Am. Soc. Mass Spectrom.* **1998**, *9*, 1204−1212.
(25) Ray, D.; Feller, D.; More, M. B.; Glendening, E. D.; Armentrout, P. B. *J. Phys. Chem.* **1996**, *100*, 16116−16125.
(26) Feller, D. *J. Phys. Chem. A* **1997**, *101*, 2723−2731.
(27) Feller, D.; Thompson, M. A.; Kendall, R. A. *J. Phys. Chem. A* **1997**, *101*, 7292−7298.
(28) Hill, S. E.; Feller, D. *Int. J. Mass Spectrom.* **2000**, *201*, 41−58.
(29) Lipkowitz, K. B. *Acc. Chem. Res.* **2000**, *33*, 555−562.
(30) Wren, A. G.; Gilbert, P. T.; Bowers, M. T. *Rev. Sci. Instrum.* **1978**, *49*, 531−536.
(31) Nagano, O.; Kobayashi, A.; Sasaki, Y. *Bull. Chem. Soc. Jpn.* **1978**, *51*, 790−793.
(32) Trueblood, K. N.; Knobler, C. B.; Lawrence, D. S.; Stevens, R. V. *J. Am. Chem. Soc.* **1982**, *104*, 1355−1362.
(33) Bovill, M. J.; Chadwick, D. J.; Sutherland, I. O.; Watkin, D. *J. Chem. Soc., Perkin Trans. 2* **1980**, 1529−1543.
(34) Meot-Ner, M. *J. Am. Chem. Soc.* **1983**, *105*, 4912−4915.
(35) Izatt, R. M.; Pawlak, K.; Bradshaw, J. S.; Bruening, R. L. *Chem. Rev.* **1991**, *91*, 1721−2085.
(36) Diederich, F.; Smithrud, D. B.; Sanford, E. M.; Wyman, T. B.; Ferguson, S. B.; Carcanague, D. R.; Chao, I.; Houk, K. N. *Acta Chem. Scand.* **1992**, *46*, 205−215.
(37) Inoue, Y.; Hakushi, T.; Liu, Y.; Tong, L. H.; Shen, B. J.; Jin, D. S. *J. Am. Chem. Soc.* **1993**, *115*, 475−481.
(38) Yi, Z. P.; Chen, H. L.; Huang, Z. Z.; Huang, Q.; Yu, J. S. *J. Chem. Soc., Perkin Trans. 2* **2000**, 121−127.
(39) Davidson, R. B.; Bradshaw, J. S.; Jones, B. A.; Dalley, N. K.; Christensen, J. J.; Izatt, R. M.; Morin, F. G.; Grant, D. M. *J. Org. Chem.* **1984**, *49*, 353−357.